Metamaterial Based Compact Branch-Line Coupler with Enhanced Bandwidth for Use in 5G Applications

Arshad K. Vallappil [1], Mohamad Kamal A. Rahim [1], Bilal A. Khawaja [2,3], and Murtala Aminu-Baba [1]

[1] Advance RF and Microwave Research Group (ARFMRG), School of Electrical Engineering
Faculty of Engineering, Universiti Teknologi Malaysia, UTM Johor Bahru, Johor, 81310, Malaysia
kvarshad2@graduate.utm.my, mdkamal@utm.my, limaminkobi@yahoo.com

[2] Faculty of Engineering, Department of Electrical Engineering
Islamic University of Madinah, Madinah, 41411, Saudi Arabia
7166@iu.edu.sa

[3] Department of Electronics and Power Engineering, PN-Engineering College (PNEC)
National University of Sciences and Technology (NUST), Habib-Rahmatullah Road, Karachi, Pakistan
khawaja.bilal@pnec.nust.edu.pk

Abstract ─ A novel compact 5G branch-line coupler (BLC) based on open-circuit coupled-lines and interdigital capacitor structure is presented in this paper. The proposed BLC shows the composite right/left handed (CRLH) metamaterial transmission-line (TL) operation. The proposed BLC is designed and simulated using CST microwave studio. The designed BLC is then fabricated using the FR4 substrate (ε_r = 4.3 and h = 1.66mm). The proposed 5G BLC with coupled-lines and the interdigital capacitor has achieved the fractional bandwidth of ~ 40.2% and the size reduction of 54% as compared to the conventional BLC. The fabricated BLC operates at 2.74 – 4.15GHz frequency band with a coupling factor of -3 ± 0.2dB and the phase difference of 88º between the output ports. The BLC measurements are performed at the operating frequency of 3.5GHz. The simulated and measured scattering parameters and phase difference results are in good agreement with each other. The proposed design is suitable for use in future butler-matrix based beamforming networks for antenna array systems in 5G wireless applications.

Index Terms ─ 5G, beamforming network, branch-line coupler, butler-matrix, Composite Right/Left Handed (CRLH) Transmission-Line (TL), interdigital capacitor.

I. INTRODUCTION

In the 5G wireless communication systems, the multi-beam and beam-scanning smart antennas [1] are playing a crucial role to get the desired output. The use of multi-beam antenna array systems and beamforming network (BFN) is an important means of achieving high directivity and improved coverages for 5G [2]-[3]. The BFNs are used for the adjustment of the amplitude and phase distribution of the multi-beam antenna array system [4]-[5]. Most studies so far have concentrated on the BFNs as a significant part of the 5G system. The butler-matrix (BM) is the most commonly used BFNs, due to its compact design, easy and low-cost fabrication process. There is no requirement of external bias in the BM operation. Moreover, it works like a reciprocal network (used for receiving/transmitting signals) and can be used for the BFN for 5G communication system. The development of the conventional BM consists of three main components, which are; 1) 3-dB couplers, 2) Crossovers and 3) 45º phase shifters. So, this paper focusses on the design of a compact branch-line coupler (BLC) with enhanced bandwidth that can achieve improved coverage for 5G application.

A quadrature coupler is one in which the input is split into two signals (usually with a goal of equal magnitudes) that are 90 degrees apart in phase. Types of quadrature couplers include BLCs (also known as quadrature-hybrid couplers), lange couplers and overlay couplers [6]. The BLCs are used in several 5G communication applications which include BM based antenna arrays, and radio frequency (RF) transceiver systems, and wideband six-port reflectometer design formed by enhanced BLCs [7]–[9]. The 5G technology has many advantages for the end-user, like providing wide coverage, high data-rates and improved spectral efficiency compared to their predecessors [9]. In addition to the above challenges, the 5G technologies have reported limited resources and the paucity of the new

Submitted On: January 20, 2020
Accepted On: April 18, 2020

structure for antenna and passive devices like BLCs, power divider, etc. [1].

In [10], the use of coupled-line unit-cells shows the same properties as dual composite right/left-handed (D-CRLH) unit-cells, and it reduces the BLC size by 52% and improves the bandwidth by 18.9%. In [11], a miniaturized BLC is developed by using the square-split ring resonators that reduces the overall area of 39.82% without much improvement in the bandwidth. In [12], a novel miniaturized BLC based on CRLH-TL structure is presented. Interdigital structure and double-spiral-defected resonant cell are used to get the properties of CRLH. In [13], the authors designed a compact structure of BLC using open stubs and meandered TL.

This paper, therefore, aims to propose, design, fabricate and characterize a new BLC, which is considered one of the main components for the construction of the 5G BM. It is envisioned that the BLC proposed in this paper can be used in the future 5G antenna array BFNs. The 3.5GHz frequency band has been chosen in this study for 5G technology [14]. Moreover, the 700 MHz, 3.5 GHz and 26/28 GHz have also been identified as potential frequency bands for the initial deployment of 5G technology in Malaysia [15]. In the next section, the design methodology of the proposed BLC will be discussed. The configuration is approximately similar to a basic BLC with the *λ/4* length with additional open-circuits coupled-lines technique, and interdigital capacitor (IDC) achieves metamaterial properties. Lai *et al.* [16] first proposed the CRLH-TL structure. The proposed 5G coupler is designed by using the CST microwave studio software which uses the finite-difference time-domain (FDTD) techniques for the 3D electromagnetic field analysis. The proposed coupler is designed using the low-cost FR4 substrate [17]. The agreement between the simulation and measured results suggest that the designed coupler performs well and can be used in the future 5G systems.

The rest of the paper is organized as follows: Section II gives a brief overview of the proposed BLC geometry and design process. The BLC fabrication and characterization are discussed in Section III. The simulated and measured results in terms of BLC parameters like reflection coefficient (S_{11}), insertion loss (S_{12}, S_{13}) and isolation loss (S_{14}) are summarized in Section IV, and then a comparison of the results is presented. Finally, Section V draws conclusions.

II. BRANCH-LINE COUPLER DESIGN

The proposed design of the new BLC is depicted in Figs. 1 (a-b). As shown in Fig. 1 (a), the BLC consists of four ports [18]. The port-1, port-2 and port-3 are input-port, through port and the coupled-port, respectively. Whereas, the port-4 is an isolated port that has no or very negligible output power. The impedance of the horizontal and vertical TL is $Z_0/\sqrt{2}$ and Z_0, respectively. Whereas, Z_0 indicate the characteristic impedance. In the proposed BLC, the value of Z_0 is chosen as 50Ω. The length of the line impedance at each branch is shown in Eq. (1). The IDC unit-cell used in the vertical arm of the BLC is shown in Fig. 1 (b). The width (W) and feed length of the BLC can be calculated by using the following equations [18] shown in Eqs. (1-7), respectively. The substrate is chosen to be FR4 with the relative permittivity (ε_r) of 4.3, and the thickness (h) of 1.66mm, respectively.

$$Feed\ length = \frac{\lambda}{4\sqrt{\varepsilon_r}} \quad . \tag{1}$$

$$A = \frac{Z_o}{60}\left(\frac{\varepsilon_r + 1}{2}\right)^{1/2} + \frac{\varepsilon_r - 1}{\varepsilon_r + 1}\left(0.23 + \frac{0.11}{\varepsilon_r}\right) = 1.5, \tag{2}$$

$$B = \frac{60\pi^2}{Z_o\sqrt{\varepsilon_r}}, \tag{3}$$

$$W/h < 2, \tag{4}$$

$$W/h = \frac{8\exp(A)}{\exp(2A) - 2} \quad , \tag{5}$$

$$W/h > 2, \tag{6}$$

$$W/h = \frac{2}{\pi}\left\{B - 1 - \ln(2B - 1)\right\} + \frac{\varepsilon_r - 1}{2\varepsilon_r}\left[\ln(B - 1) + 0.39 - \frac{0.61}{\varepsilon_r}\right]. \tag{7}$$

The value of A is 1.5 and 1.1 by substituting impedance equal to 50Ω and 35Ω, respectively for vertical and horizontal arms of the BLC. Based on Eq. (1-7), the BLC-TL width (W_{35}) and (W_{50}) is optimized to 5mm and 2.8mm for the fabrication of BLC, as shown in Fig. 1 (a), respectively. The dimensions of the horizontal and vertical IDC unit-cell are summarized in Table 1. The difference of dimensions in the horizontal and vertical unit-cell finger length is due to the impedance matching and the S-matrix requirements for the four-port BLC [18]. Figure 1 (b) also shows that the gap *'s'* between the fingers and at the end of the fingers are same. The fingers have a width of '*m*', and length '*l'* which are also specified. The top surface of the substrate is a copper conductor with a thickness of 0.035mm.

The substrate properties will also affect the BLC performance. Due to the ease of design and fabrication, the IDC often uses planar microstrip TL. Many authors have studied the properties of this type of capacitor [19]–[23]. There are many assumptions made for the calculation of capacitance, some of which are: (1) finger

and gap width are considered (2) capacitance also depends on the number of fingers (3) the capacitor dimensions are much less than a quarter wavelength; (4) metallization thickness and (5) the capacitance is neglected at the end of the finger. An enhanced model where the capacitor is divided into its core components is studied briefly in [24].

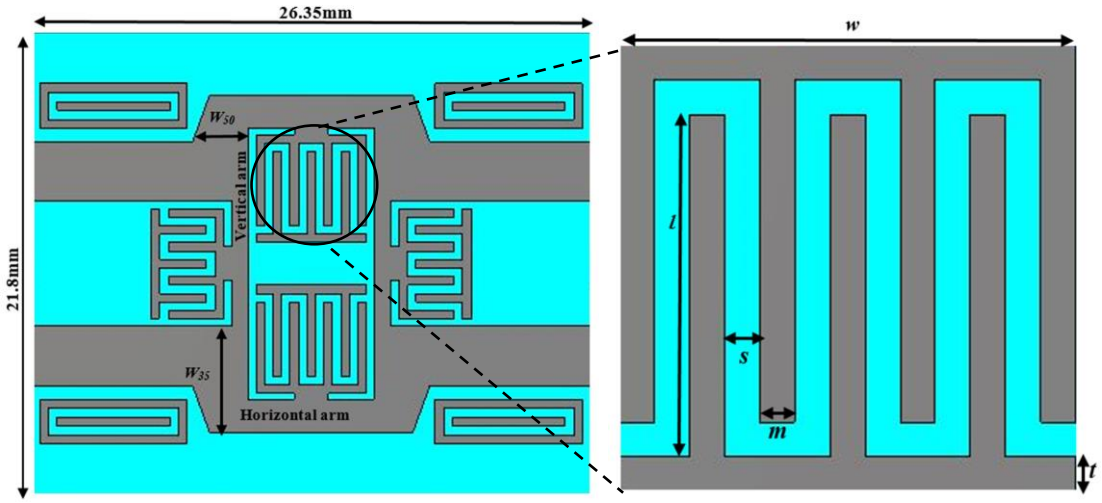

(a) (b)

Fig. 1. (a) Proposed BLC showing Interdigital capacitor unit-cell and open-circuits coupled-lines, and (b) zoom-in of IDC unit-cell.

Table 1: Dimensions of horizontal and vertical IDC unit-cell

Description	Notation	Dimension (mm)
Horizontal Arm		
Finger Width	*m*	0.4
Finger Length	*l*	3.9
Width of IDC	*w*	5.2
Finger Gap	*s*	0.4
Exterior Finger Width	*t*	0.4
Vertical Arm		
Finger Width	*m*	0.4
Finger Length	*l*	2.2
Width of IDC	*w*	5.2
Finger Gap	*s*	0.4
Exterior Finger Width	*t*	0.4

Figures 2 (a-b) shows the proposed equivalent circuit model of the IDC. Alley *et al.* [19] have developed the most popular model. The effect of interdigital fingers capacitance is taken into account in this model. The total capacitance is given by Eq. (8) [24]:

$$C = (\varepsilon_r + 1) l \left[(N-3)A_1 + A_2\right] \text{(pF)}. \quad (8)$$

In Eq. (8), N represents the number of fingers and the relative permittivity of substrate material represented as ε_r. The constant A_1 and A_2 in Eq. (8) are represented by Eqs. (9-10) [25], respectively:

$$A_1 = 4.409 \tanh\left[0.55\left(\frac{h}{w}\right)^{0.45}\right] \times 10^{-6} \text{(pF/μm)}, \quad (9)$$

$$A_2 = 9.92 \tanh\left[0.52\left(\frac{h}{w}\right)^{0.5}\right] \times 10^{-6} \text{(pF/μm)}. \quad (10)$$

The constant A_1 and A_2 represented IDC interior and exterior finger in terms of h and w. The w is the width of the overall IDC conductor, and the h represents the thickness of the substrate material. Based on Eqs. (8-10), the capacitance of IDC is equal to 0.14pF. Figures 2 (a-b) represent the IDC's lumped equivalent circuits (EC) for the low- and high-frequency applications, respectively**.** Finally, the series parasitic resistance due to conductor loss is given by Eq. (11):

$$R = \frac{4}{3}\frac{l}{mN} R_s \ (\Omega). \quad (11)$$

Where, R_s is the sheet resistivity of the conductor. The capacitance (C_s) and inductance (L) in eq. (12-13) are calculated for the $m/h << 1$ approximations. The magnetic field lines are also considered not to loop around each finger, but to loop around the cross-section of the interdigital width, as shown previously in Fig. 2(a). The c indicates the velocity of light in free space.The L and C_s are represented as [22]:

$$L = \frac{Z_0\sqrt{\varepsilon_{eff}}}{c} l \text{ (H)}, \quad (12)$$

$$C_S = \frac{1}{2}\frac{\sqrt{\varepsilon_{eff}}}{Z_0 c} l \text{ (F)}. \quad (13)$$

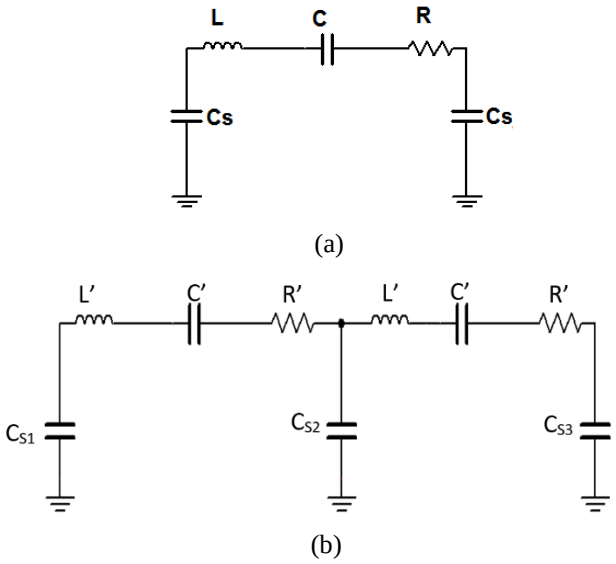

Fig. 2. EC of the IDC: (a) low frequency and (b) high frequency model, respectively.

The parameters *l* and *w* of the IDC unit-cell, as shown in Fig. 1 (b) are calculated in multiple steps which are described below by using Eqs. (14-15), respectively [26]:

Step-1: Choose center frequency (f_o) = 3.5 GHz.

Step-2: Calculate the width of IDC required to achieve BLC horizontal arm impedance of $Z_o/\sqrt{2}$. Based on Eqs. (2-7), the value of '*w*' is found to be 5.2 mm.

Step-3: Set the number of fingers, '$N = 7$' (as per BLC design shown in Figs. 1 (a-b)). Then, by using Eq. (14), determine the required parameter '*m*' and '*s* = 2m / 3':

$$m \approx \frac{w}{\left(\frac{5N}{3} - \frac{2}{3}\right)}. \tag{14}$$

Step-4: Optimize the value of '*m*' and '*s*' to 0.4mm.

Step-5: Calculate the value of '*l*' and optimize it to 3.9mm by using Eq. (15):

$$l \approx \frac{\lambda_g}{8} \approx \frac{c}{8f_o\sqrt{\varepsilon_r}}. \tag{15}$$

The different techniques such as double quarter-wave transformer, series open-circuited stubs, open-circuited capacitively coupled lines, and arbitrary power division ratio have been implemented in conventional BLC design to overcome the bandwidth limitation. From these techniques, capacitively coupled *λ/4* open-circuited lines achieve a much improved fractional bandwidth of 63% [27]. So, in this work, it was decided to insert four capacitively coupled open-circuited *λ/4* lines at each port of the proposed BLC by adopting proper characteristic impedances for arbitrary power coupling. This will provide wide bandwidth with DC block capability and flat coupling characteristics [28]. The wideband characteristics of BLC can be analyzed by the equivalent admittance approach of the matched BLC and by the characteristics impedance calculation of the coupled lines as described in [29]. The dimensions of the coupled-lines are summarised in Fig. 3. The IDC make a shunt capacitor, and the coupled lines generate series gap capacitance with respect to the TL, which is acting as an inductor. Therefore, it has series and parallel LC circuit that makes a metamaterial TL.

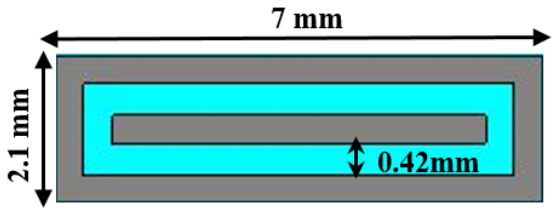

Fig. 3. Geometry of an open-circuit coupled-line used in the proposed BLC design with its dimensions

III. BLC FABRICATION AND CHARACTERISATION

The proposed and designed BLC is then fabricated using the FR4 substrate. Figure 4 (a) shows the fabricated BLC PCB and its dimensions, which are 27mm x 23mm, respectively and highlight the compact size of the BLC. The SMA connectors are then used with the fabricated BLC prototype for measurements. The fabricated BLC with detailed port information and dimensions are shown in Fig. 4 (b). It is important to note in Fig. 4 (b) that the central conductor of the SMA connector is only soldered to the transmission line for the measurement purposes. The S-parameter measurements of the fabricated BLC are then performed using Keysight (Agilent Technologies) FieldFox N9925A vector network analyzer (VNA).

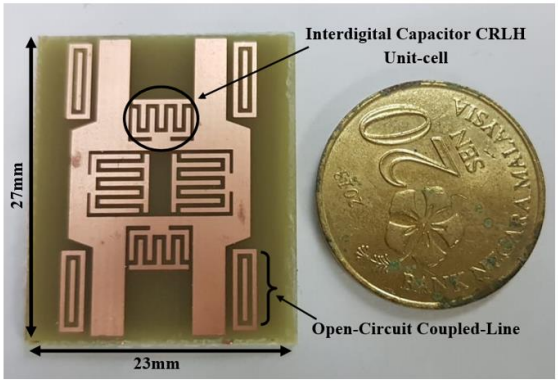

(a)

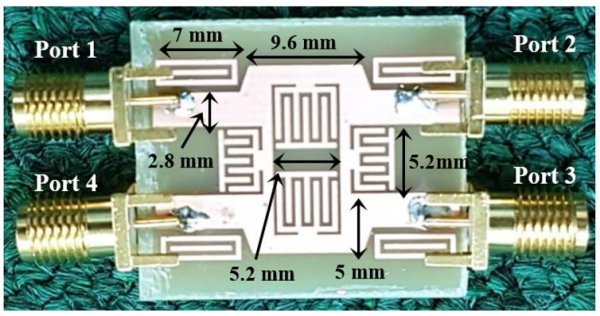

(b)

Fig. 4. FR4 substrate based fabricated prototype of the proposed BLC: (a) without connectors and (b) corresponding BLC ports and PCB dimensions are shown with SMA connectors

IV. RESULTS AND DISCUSSION

This section discusses the simulated and measured results of the BLC. Figure 5 (b) and Fig. 6, illustrate the performance of the proposed 5G BLC in terms of S-parameters and phase differences between the output ports, respectively. The simulation results in Fig. 5 (b), show that the proposed BLC is operating between 2.87GHz to 4.17GHz frequency band with a coupling factor of -3dB, respectively. The proposed simulated BLC return-loss (S_{11}) and isolation loss (S_{14}) characteristics were achieved better than 10dB and the bandwidth of 37.2% at 3.5GHz as compared to the conventional BLC result shown in Fig. 5 (a). Meanwhile, the proposed BLC design consideration in terms of insertion loss (S_{12}) and the coupling loss (S_{13}) should be -3dB to achieve equal power splitting across the port-2 and port-3. The simulated S_{12} and S_{13} results, as shown in Fig. 5 (b) are -3.04dB and -3.17 dB, respectively, also lying in the same frequency range. The insertion and coupling loss error (LE) is 0.04dB and 0.17dB, respectively, for the desired value of -3dB.

The phase difference between port-3 and port-2 should be 90° as per the design consideration of the proposed BLC. The comparison of simulated and measured results are shown in Fig. 6. It can be observed from Fig. 6 that when port-1 is excited, the simulated phase difference between port-3 and port-2 are 169.37° (S_{13}) and 78.47° (S_{12}), respectively, at 3.5GHz frequency band. In the simulation results, the phase difference between port-3 and port-2 is 90.9° as per the Eq. (16). So, the phase error is 0.9° with respect to the desired value of 90°:

$$\angle S_{13} - \angle S_{12} = \varphi. \quad (16)$$

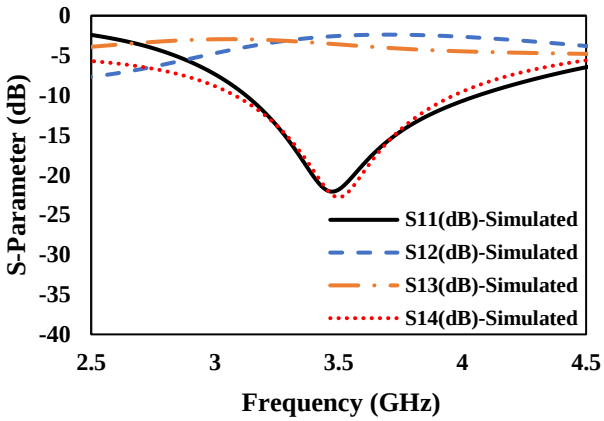

(a)

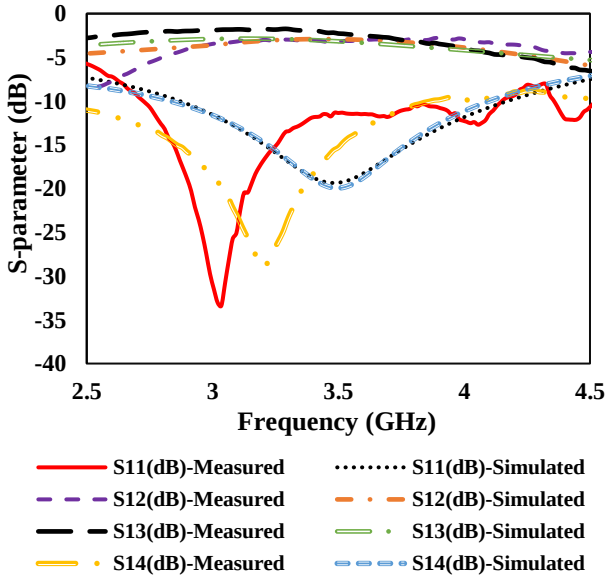

(b)

Fig. 5. S-Parameter response of: (a) conventional BLC (simulated response), and (b) proposed designed and fabricate BLC (both simulated and measured response).

The designed BLC has an overall area of 21.8mm x 26.65mm = 580.97 mm^2. Since, the conventional BLC area is 30mm x 41.7mm = 1251 mm^2 at 3.5 GHz, without degradation in performance, the proposed BLC only occupies 46% of the conventional design area. Figure 5 (a) shows the conventional BLC S-Parameter response. Compared to the conventional BLC [18], the proposed design is highly competitive, as shown in Table 2.

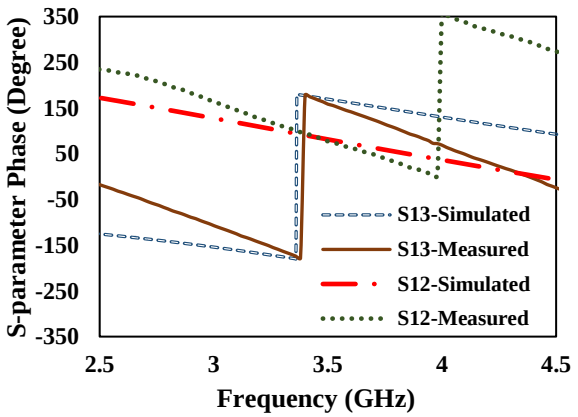

Fig. 6. Simulated and measured phase difference between port-2 and port-3.

Table 2: Results comparison of simulated conventional BLC design with proposed simulated and measured BLC Response at 3.5GHz

Parameter	Conventional BLC (Simulated)	Proposed BLC Design (Simulated)	Proposed BLC Design (Measured)
S_{11}	-24dB	-19dB	-12dB
S_{12}	-2.5dB	-3.04dB	-3.19dB
S_{13}	-3.6dB	-3.17dB	-2.8dB
S_{14}	-17dB	-19dB	-15.2dB
Phase Difference	89°	90.9°	88°
Bandwidth **@ S_{11} below -10dB**	3.1 GHz to 4.06 GHz	2.87 GHz to 4.17 GHz	2.74 GHz to 4.15 GHz
Size	30mm x 41.7mm	21.8mm x 26.65mm	23mm x 27mm
Percentage Reduction	54%		

A comparison between the simulated and measured results is shown in Fig. 5 (b) for the S_{11}, S_{12}, S_{13} and S_{14} magnitudes, and in Fig. 6 for the S_{12} and S_{13} phases, respectively. The proposed BLC shows good agreement between the simulated and measured results. The measured S_{11} is better than -10dB between 2.74 - 4.15 GHz frequency band, with a 40.2% relative bandwidth. The isolation loss (S_{14}) is also better than -10dB between 2.5 GHz to 4.1 GHz frequency band. Meanwhile, the performance of the insertion loss (S_{12}) and the coupling (S_{13}) are at -3.2dB and -2.8dB respectively, also lying in the same frequency range. So that the insertion and coupling LE is ±0.2dB with respect to the desired value. As depicted in Fig. 6, the measured phase of port-3 and port-2 at 3.5GHz is 166.4° (S_{13}) and 78.4° (S_{12}) respectively, when port-1 is excited. The BLC has a measured phase difference of 88° between Port-2 and Port-3 as per the Eq. (14). So, the phase error is 2° with respect to the desired value.

In the comparison between the simulated and measured results shown in Fig. 5 (b) and Fig. 6, there is a small shift in the centre frequency, but the range of frequency lies in the same frequency band between 2.74GHz to 4.15GHz, respectively. The dielectric loss tangent (tan δ) of the simulated FR-4 substrate is around 0.025, whereas for the fabricated FR-4 substrate based prototype is around 0.019. Because of this variation in the lossy FR4 substrate properties [30], there is a shift in the centre frequency, coupling and insertion LE of 0.2dB with respect to the standard value of 3dB, and the phase difference error (PDE) of 2^0. The dielectric constant of the FR-4 is also frequency-dependent and varies with the frequency. In the future, this frequency shift problem, LE, and the PDE can be improved by using a low-loss substrate.

A comparison of the proposed BLC with the previously published work related to BLC is summarized in Table 3. The researchers are attempting to either enhance the bandwidth or to minimize the size of the BLC in most of the design described in Table 3. The proposed work shows the bandwidth enhancement and minimize the size of the BLC together, which is considered as the main requirement for the design of 5G system. Moreover, the LE and PDE are also very small as compared to the previous designs.

Table. 3: Comparison of Proposed BLC design with the existing designs available in the literature

Operating Freq. (GHz)	Bandwidth (S_{11} = -10dB)	Size Reduction	Loss Error (dB)	PD Error (Deg)	Ref. / Year
3.22	5%	54.7%	± 1dB	-3°	[36] / 2013
3.5	6.57%	67 %	± 1.7dB	-4°	[33] / 2015
3.5	34%	63%	± 0.9dB	±5°	[34] / 2015
3.5	14.6%	61.76%	± 0.9dB	≈1°	[31] / 2016
3.5	≈17%	≈75%	± 0.5dB	-1.7°	[37] / 2016
3	13.3%	55%	± 0.3dB	1°	[32] / 2018
3.8	15.7%	40%	± 0.5dB	-2.5°	[35] / 2019
3.5	40.2%	54%	± 0.2dB	-2 °	[This work] / 2020

From Table 3, it is important to note that LE refers to the difference between the insertion loss/coupling loss with the desired value of -3dB. Also, the PDE refers to the phase difference between port-3 and port-2 of the BLC with the desired value of 90°.

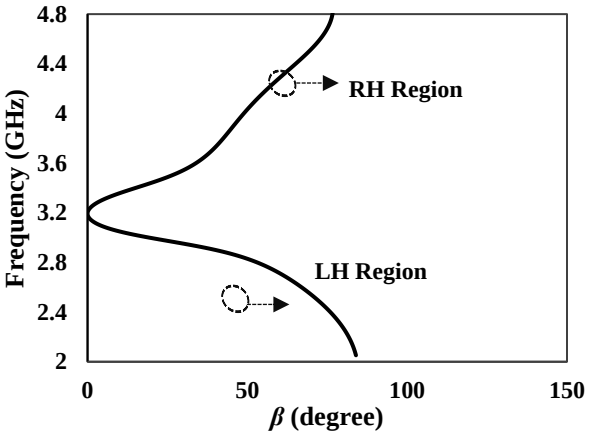

Fig. 7. Dispersion diagram of the proposed BLC.

Figure 7 shows the dispersion diagram of the proposed BLC. The dispersion diagram is plotted for the frequency and absolute value of β. The value of β is calculated using the S-parameter value, and it clearly shows that high frequency supports the forward wave and low-frequency support backward wave. Hence, the proposed BLC is designed to work in the right-hand (RH) region from above 3.2 GHz and left-hand (LH) region from below 3.2GHz. This indicates that the proposed BLC is a CRLH metamaterial TL [19],[38]. The main requirement for 5G technology is wide bandwidth and compact size of the components [39]. The CRLH-TL exhibit a bandpass behavior between the RH and LH regions, which shows improved bandwidth, as shown in Fig. 7 and the compact size of the proposed BLC.

V. CONCLUSION

A new BLC was proposed in this paper based on the interdigital capacitor unit-cell and open coupled lines technique that shows metamaterial TL properties. The simulated and measured results of the proposed BLC showed that the coupler has excellent S-parameter and phase difference performances at the desired operating frequency of 3.5GHz. The BLC is operating at the frequency band of 2.74 GHz - 4.15 GHz. The proposed BLC design is then fabricated, and it demonstrates a high fractional bandwidth of up to 40.2%. This article explained the compact and wide-band BLC has a good profile that is 54% less in size than conventional BLCs. The proposed BLC is potentially suitable to be used later in the butler-matrix based array antenna system for the 5G applications [40]. The structure can be integrated to form a compact and wideband butler-matrix for future array antenna beamforming systems.

ACKNOWLEDGMENT

The authors would like to thank the Ministry of Higher Education (MOHE), School of Postgraduate Studies (SPS), Research Management Centre, Advanced RF and Microwave Research Group, School of Electrical Engineering, and Universiti Teknologi Malaysia (UTM), Johor Bahru, for the support of the research under Grant 09G19 and 06G15.

REFERENCES

[1] W. Hong, et al., "Multibeam antenna technologies for 5g wireless communications," *IEEE Transactions on Antennas and Propagation*, vol. 65, no. 12, pp. 6231-6249, Dec. 2017.

[2] Y. Cao, K. S. Chin, W. Che, W. Yang, and E. S. Li, "A compact 38 ghz multibeam antenna array with multifolded butler matrix for 5g applications," *IEEE Antennas and Wireless Propagation Letters*, vol. 16, pp. 2996-2999, 2017.

[3] J. Zhang, X. Ge, Q. Li, M. Guizani, and Y. Zhang, "5g millimeter-wave antenna array: design and challenges," *IEEE Wireless Communications*, vol. 24, no. 2, pp. 106-112, Apr. 2017.

[4] T. A. Denidni and T. E. Libar, "Wide band four-port butler matrix for switched multibeam antenna arrays," *14th IEEE Proceedings on Personal, Indoor and Mobile Radio Communications, PIMRC 2003*, vol. 3, pp. 2461-2464 ,2003.

[5] C. Chen, H. Wu, and W. Wu, "Design and implementation of a compact planar 4 × 4 microstrip butler matrix for wideband application," *Progress In Electromagnetics Research C*, vol. 24, pp. 13, 2011.

[6] "Microwaves101 | Quadrature Couplers." [Online]. Available: https://www.microwaves101.com/encyclopedias/quadrature-couplers

[7] N. A. M. Shukor, N. Seman, and D. N. A. Zaidel, "Wideband six-port reflectometer design formed by enhanced branch-line couplers," *IEEE Asia-Pacific Conference on Applied Electromagnetics (Apace)*, pp. 63-66, 2014.

[8] S. I. Orakwue, R. Ngah, T. A. Rahman, and H. M. R. Al-Khafaji, "A 4 × 4 butler matrix for 28 ghz switched multi-beam antenna," *Int. J. Eng. Technol.*, vol. 7, no. 2, pp. 7, 2015.

[9] S. N. A. M. Ghazali, N. Seman, M. Rahim, S. Abdul Rahim, and R. Che Yob, "Design of complex ratio measuring unit (crmu) for 2 to 6 GHz WiMAX applications," *Asia-Pacific Microwave Conference Proceedings*, pp. 1271-1273, 2012.

[10] S. Gomha, E.-S. El-Rabaie, A.-A. Shalaby, and A. Elkorany, "Design of new compact branch-line coupler using coupled line dual composite right/left-handed unit cells," *J. Optoelectron. Adv. Mater.*, vol. 9, pp. 836-841, June 2015.

[11] Y. L. Li, Q. S. Liu, S. Sun, and S. S. Gao, "A miniaturised butler matrix based on patch hybrid couplers with cross slots," *IEEE Antennas and Propagation Society International Symposium*

(APSURSI), pp. 2145-2146, 2013.

[12] L. Geng, G.-M. Wang, P. Peng, and Y.-W. Wang, "Design of miniaturized branch-line coupler based on novel composite right/left-handed transmission line structure," *IEEE International Conference on Computational Electromagnetics (ICCEM)*, pp. 1-3, 2019.

[13] S. Gomha, E.-S. M. El-Rabaie, and A. A. T. Shalaby, "Miniaturization of branch-line couplers using open stubs and stepped impedance unit cells with meandering transmission lines," *Circuits Syst.*, vol. 1, pp. 14, 2014.

[14] Study on Implications of 5G Deployment on Future BusinessModels." [Online]. Available: https://berec.europa.eu/eng/document_register/subject_matter/berec/reports/8008-study-on-implications-of-5g-deployment-on-future-business-models

[15] "Press Release: Final Report on Allocation of Spectrum Bands for Mobile Broadband Service in Malaysia." [Online]. Available: https://www.mcmc.gov.my/en/media/press-releases/final-report-on-allocation-of-spectrum-bands-for-m

[16] A. Lai, T. Itoh, and C. Caloz, "Composite right/left-handed transmission line metamaterials," *IEEE Microw. Mag.*, vol. 5, pp. 34-50, Sep. 2004.

[17] "F4B material datasheet." [Online]. Available: http://oneseine.com/edownload/12.html

[18] D. M. Pozar, *Microwave Engineering*. 3rd ed., John Wiley and Sons, 2005.

[19] G. D. Alley, "Interdigital capacitors and their application to lumped-element microwave integrated circuits," *IEEE Trans. Microw. Theory Tech.*, vol. 18, no. 12, pp. 1028-1033, Dec. 1970.

[20] D. Lacombe and J. Cohen, "Octave-band microstrip dc blocks (short papers)," *IEEE Trans. Microw. Theory Tech.*, vol. 20, no. 8, pp. 555-556, Aug. 1972.

[21] J. L. Hobdell, "Optimization of interdigital capacitors," *IEEE Trans. Microw. Theory Tech.*, vol. 27, no. 9, pp. 788-791, Sep. 1979.

[22] R. Esfandiari, D. W. Maki, and M. Siracusa, "Design of interdigitated capacitors and their application to gallium arsenide monolithic filters," *IEEE Trans. Microw. Theory Tech*., vol. 31, no. 1, pp. 57-64, Jan. 1983.

[23] X. Y. She and Y. L. Chow, "Interdigital microstrip capacitor as a four-port network," *Antennas Propag. IEEE Proc. H - Microw.*, vol. 133, no. 3, pp. 191-197, June 1986.

[24] I. J. Bahl and P. Bhartia, *Microwave Solid State Circuit Design*, Wiley, New York, 1988.

[25] R. Siragusa, H. V. Nguyen, P. Lemaître-Auger, S. Tedjini, and C. Caloz, "Modeling and synthesis of the interdigital/stub composite right/left-handed artificial transmission line," *Int. J. RF Microw. Comput.-Aided Eng.*, vol. 19, no. 5, pp. 549-560, Sep. 2009.

[26] C. Caloz and T. Itoh, *Electromagnetic Metamaterials: Transmission line Theory and Microwave Applications*, Wiley and IEEE Press, Hoboken, NJ, 2005.

[27] W. Arriola and I. S. Kim. "Wideband branch line coupler with arbitrary coupling ratio," *Asia-Pacific Microwave Conference*, Melbourne, VIC, USA, Dec. 2011.

[28] M. W. Sabri, N. A. Murad, and M. K. A. Rahim, "Wideband branch line coupler with open circuit coupled lines," *Int. J. Electr. Comput. Eng. IJECE*, vol. 7, no. 2, pp. 888-893, Apr. 2017.

[29] W. A. Arriola, J. Y. Lee, and I. S. Kim. "Wideband 3 db branch line coupler based on λ/4 open circuited coupled lines," *IEEE Microw. & Wireless Comp. Lett.*, vol. 21, no. 9, pp. 486-488, 2011.

[30] D. C. Nascimento and J. C. Da S. Lacava, "Design of low-cost probe-fed microstrip antennas," *Microstrip Antennas*, Apr. 2011.

[31] S. Azzeddine, et al., "A novel design of miniature coupler for wimax applications," *Int. J. Microw. and Opti. Tech.*, vol. 11, pp. 80-85, 2016.

[32] Z. Cai, et al., "Miniaturized branch-line coupler using delta stubs," *2018 Cross Strait Quad-Regional Radio Science and Wireless Technology Conference (CSQRWC)*, Xuzhou, China, July 2018.

[33] Y. Cao, J. Wen, H. Hong, and J. Liu, "Design of planar dual-band branch-line coupler with π-shaped coupled lines" *Progress In Electromagnetics Research*, vol. 55, pp. 113-120, 2015.

[34] N. M. Jizat, N. M. Isa, J. S. Francisca, and S. K. A. Rahim, "3-dB branch-line coupler using coupled line radial stub with no restriction on coupling power," *2015 IEEE 12th Malaysia International Conference on Communications (MICC)*, Kuching, Malaysia, Nov. 2015.

[35] M. H. Seko and F. S. Correra, "Dual-band branch-line coupler with shorted stepped-impedance stubs arranged in a π-shaped topology," *Microw. and Opt. Tech. Lett*, vol. 61, no. 5, pp. 1154-1160, May 2019.

[36] X.-K. Zhang, et al., "Design of miniaturized branch-line coupler based on novel center-symmetrical spiral-interdigital resonators," *IEEE 2013 Cross Strait Quad-Regional Radio Science and Wireless Tech. Conference*, Chengdu, China, July 2013.

[37] H. Zhang, W. Kang, and W. Wu, "A novel compact dual-band branch-line coupler with cross-shaped stubs," *IEEE International Conference on Ubiquitous Wireless Broadband (ICUWB), Nanjing, China*, Oct. 2016.

[38] A. Rennings, T. Liebig, S. Otto, C. Caloz, and I. Wolff, "Highly directive resonator antennas based on composite right/left-handed (crlh) transmission

lines," *2nd International ITG Conference on Antennas*, pp. 190-194, 2007.

[39] H. Yu, H. Lee, and H. Jeon, "What is 5g? emerging 5g mobile services and network requirements," *Sustainability*, vol. 9, no. 10, pp. 1848, 2017.

[40] S. Trinh-Van, J. M. Lee, Y. Yang, K. Lee, and K. C. Hwang, "A sidelobe-reduced, four-beam array antenna fed by a modified 4× 4 butler matrix for 5g applications," *IEEE Trans. on Antennas and Prop.*, vol. 67, no. 7, pp. 4528-4536, July 2019.

Arshad Karimbu Vallappil received the B.Tech degree in Electronics & Communication Engineering from the University of Calicut, Kerala, India, in 2009 and M.Tech degree in Electronics Engineering from Pondicherry University, Puducherry, India in 2013. Currently, he is pursuing Ph.D. in Electrical Engineering from University Teknologi Malaysia, Malaysia.

Mohamad Kamal A. Rahim received the B.Eng. degree in Electrical and Electronic Engineering from the University of Strathclyde, U.K., in 1987, M.Sc. degree in Engineering from the University of New South Wales, Australia, in 1992, and the Ph.D. degree in the field of Wideband Active Antenna from the University of Birmingham, U.K., in 2003. From 1992 to 1999, he was a Lecturer with the Faculty of Electrical Engineering, Universiti Teknologi Malaysia (UTM), where he was a Senior Lecturer with the Department of Communication Engineering from 2005 to 2007. He is currently a Professor with UTM, Malaysia.

Bilal A. Khawaja received the B.S. degree in Computer Engineering from Sir Syed University of Engineering and Technology, Karachi, Pakistan, in 2002, the M.Sc. degree in Communication Engineering and Signal Processing from the University of Plymouth, Plymouth, U.K., in 2005, and the Ph.D. degree in Electrical Engineering from the University of Bristol, Bristol, U.K. in 2010. From 2010 to 2016, he was working as an Assistant Professor in Department of Electronics and Power Engineering, PN-Engineering College, National University of Science and Technology (NUST), Karachi, Pakistan. Currently, he is an Associate Professor with the Department of Electrical Engineering, Faculty of Engineering, Islamic University of Madina, Madina, Saudi Arabia. His current research interests include Antennas and Antenna Array design and characterization for the Wi-Fi, IoT, UAVs / FANETs and 5G Systems.

Murtala Aminu-baba obtained his first degree in 2010 from Abubakar Tafawa University Bauchi, Nigeria in Electrical/Electronic Engineering. He further received his MSc. degree in IT from the University of Wolverhampton, U.K, in 2013. He is currently pursuing his Ph.D. in the field of metamaterial antenna design for MIMO applications.